Astragalus Polysaccharide Inhibits Ionizing Radiation-Induced Bystander Effects by Regulating MAPK/NF-κB Signaling Pathway in Bone Mesenchymal Stem Cells (BMSCs)

Authors' Contribution:
Study Design A
Data Collection B
Statistical Analysis C
Data Interpretation D
Manuscript Preparation E
Literature Search F
Funds Collection G

CE 1 **Liying Zhang***
CE 1 **Yali Luo***
C 1 **Zhiwei Lu**
C 2 **Jinpeng He**
C 1 **Lei Wang**
B 1 **Lixin Zhang**
B 1 **Yiming Zhang**
AE 1,3 **Yongqi Liu**

1 Provincial-Level Key Laboratory for Molecular Medicine of Major Diseases and The Prevention and Treatment with Traditional Chinese Medicine Research in Gansu Colleges and Universities, Gansu University of Traditional Chinese Medicine, Lanzhou, Gansu, P.R. China
2 Key Laboratory of Space Radiobiology of Gansu Province and Key Laboratory of Heavy Ion Radiation Biology and Medicine of Chinese Academy of Sciences, Institute of Modern Physics, Chinese Academy of Sciences, Lanzhou, Gansu, P.R. China
3 Key Laboratory for Transfer of Dunhuang Medicine at the Provincial and Ministerial Level, Gansu University of Traditional Chinese Medicine, Lanzhou, Gansu, P.R. China

Corresponding Author:
Source of support:

* These authors contributed equally to this work
Yongqi Liu, e-mail: liuyongqi73@163.com
This study was supported by a grant from the National Natural Science Foundation of China [grant number 81473457]

Background:
This study investigated the effect of Astragalus polysaccharides (APS) on radiation-induced bystander effects (RIBE) in human bone mesenchymal stem cells (BMSCs) induced by irradiated A549 cells.

Material/Methods:
A549 cells were irradiated with 2 Gy X-rays to obtain conditioned medium. BMSCs were incubated with the conditioned medium or APS. The levels of reactive oxygen species (ROS) and TGF-β were detected by ELISA. Cell survival, genomic instability, and DNA damages were detected by CCK-8 assay, colony formation assay, the micronucleus test and immunofluorescence assay, respectively. The protein and phosphorylation protein expression of p38, c-Jun N-terminal kinase (JNK), extracellular regulated protein kinase (ERK1/2), P65, and cyclooxygenase-2 (COX-2) in bystander effect cells were detected by Western blot.

Results:
The expression of COX-2 and ROS increased following stimulation with conditioned medium; this effect was inhibited by pre-exposing the cells to APS. BMSCs growth and colony formation rate decreased following stimulation with conditioned medium; this effect was suppressed by pre-exposing the cells to APS. In addition, the micronucleus rate and 53BP1 foci number increased after treatment with conditioned medium; this increase in BMSCs was inhibited by APS. The levels of phosphorylated p38, JNK, ERK1/2, NF-κB P65, and COX-2 proteins were increased by conditioned medium but were decreased by pre-treatment with APS.

Conclusions:
RIBE in BMSCs induced by the irradiated A549 was mediated by the ROS in the conditioned medium and might be related to MAPK/NF-κB signal pathways in BMSCs. APS may block RIBE through regulating the MAPK/NF-κB pathway.

MeSH Keywords:
Bystander Effect • Mesenchymal Stromal Cells • Polysaccharides

Abbreviations:
APS – Astragalus polysaccharides; **RIBE** – radiation-induced bystander effects; **BMSCs** – bone mesenchymal stem cells; **ROS** – reactive oxygen species; **JNK** – Jun N-terminal kinase; **ERK1/2** – extracellular regulated protein kinases; **COX-2** – cyclooxygenase-2; **DSB** – DNA double-strand breaks

Full-text PDF:
https://www.medscimonit.com/abstract/index/idArt/909153

📄 3295   🗐 —   📊 6   📖 64

Background

Radiotherapy can significantly decrease the recurrence rate of lung cancer, especially that of non-small cell lung cancer at early stage [1]. However, the radiation-induced bystander effects (RIBE) are one of the major problems of radiotherapy [2]. RIBE is a phenomenon in which unirradiated cells exhibit irradiated effects as a result of receiving signals from nearby irradiated cells [3]. Studies demonstrate that soluble cytokines induced by radiation [4] can promote the release of ROS, which can induce DNA double-strand breaks (DSB) and genomic instability [5]. Thus, the neighboring cells or distant tissues outside the direct radiation exposure field present the same biological endpoints of radiation such as DNA damage, [6] chromosome aberrations, [7] cell death [8], and gene mutation [9].

BMSCs are multipotent cells with self-replicative, regenerative, and immunomodulatory properties [10–12] and they can migrate to the inflammation site, injury tissue, and even tumors, including lung cancer [13–16]. Notably, dysregulated expression of the oncogenes and tumor suppressor genes and the chromosomal abnormalities were observed in BMSCs that were co-cultured with tumor cells [17,18], indicating that the BMSCs may be damaged by the adverse environment. However, the possible damage to BMSCs during the radiotherapy of lung cancer is unclear so far.

Astragalus polysaccharides (APS), a major active ingredient of *Astragalus membranaceus* [19], has various bioactivities, such as immunoregulatory, antiviral, hypoglycemic, antioxidant, and anti-tumor properties [20,21]. The anti-inflammatory properties of APS as well as its protective effects on various organs [22,23] and its anti-oxidation effects have been investigated extensively [24–26]. During the radiotherapy of lung cancer, the anti-apoptotic effects of APS were observed [27]. However, its protective effects against damage to BMSCs induced by RIBE have not been reported.

In the present study, A549 cells were irradiated with X-rays and then co-cultured with BMSCs to induce RIBE in BMSCs. The effects of APS on proliferation, genomic instability, and DNA damages of BMSCs in RIBE were investigated. The underlying mechanisms were analyzed and discussed.

Material and Methods

Cell lines and cell culture

BMSCs (ScienCell Research Laboratories, San Diego, CA, USA) were cultured in mesenchymal stem cell medium (ScienCell Research Laboratories) and maintained in a 5% CO_2 humidified incubator (Thermo Scientific, NC, USA) at 37°C. A549 cells (Cell Bank, Shanghai Institutes for Biological Sciences, Chinese Academy of Sciences; Cat# TCHu150, China) were cultured in DMEM/F-12 medium (Gibco, 12500-062, USA) supplemented with 10% fetal bovine serum (Hyclone, USA), 100 units/mL penicillin, and 100 mg/mL streptomycin and maintained in a 5% CO_2 humidified incubator (Thermo Scientific) at 37°C.

Irradiation

A549 cells were irradiated in a laboratory RX-650 X-ray system (Faxitron, Tucson, AZ, USA). The X-ray energy was kept at 100 kVp and the dose rate was about 0.6 Gy/min (100 KeV, 5 mA). The total absorbed dose was 2 Gy. All irradiations were performed at room temperature.

Collection of conditioned medium

A549 cells were cultured to 80% confluency and the medium was replaced with mesenchymal stem cell medium before irradiation. Medium was harvested at 0 h, 0.5 h, 2 h, 3 h, 6 h, 8 h, and 12 h after irradiation. Conditioned medium was obtained after centrifugation at 1000 rpm for 5 min.

Groups

BMSCs were divided into 4 groups. BMSCs cultured with mesenchymal stem cell medium served as the blank control group. BMSCs cultured with mesenchymal stem cell medium supplemented with 50 g/mL APS (Shanghai Yuanye Biological Technology Company ZD1219LA13, China; with purity >98%) for 3 d served as the APS medium group (APS group). BMSCs cultured with conditioned medium (collected at 3 h after irradiation) served as the conditioned medium group (CM group). BMSCs cultured with mesenchymal stem cell medium rich in 50 g/mL APS for 3 d and then cultured with conditioned medium (collected at 3 h after irradiation) served as the APS and conditioned medium group (APS+CM group). The culture supernatant of each experiment group was collected at 0 h, 3 h, 6 h, 9 h, 12 h, 15 h, and 18 h after co-culturing with conditioned medium.

CCK-8 assay

The CCK-8 assay kit (Dojindo, Japan) was used to detect cell viability according to the manufacturer's instructions. After treatment for 3 d with different media, cells were seeded onto 96-well plates at a density of 2000 cells per well. Then, cell viability was detected at 1 d, 2 d, 3 d, 4 d, and 5 d. Then, 20 µL of CCK-8 (10% in culture medium) were added to cells at each time point. Cells were then incubated for 4 h at 37°C. After agitation for 10 min on a shaker, absorbance at 450 nm was read using a microplate reader (Tecan Infinite M200; Salzburg, Austria).

Cell colony formation assay

After treatment, BMSCs in single-cell suspension were seeded into 60-mm culture dishes and cultured with 5% CO_2 at 37°C. The total number of the cells were 100 in each dish. The cells were cultured for 14 d to form colonies. Colonies were fixed in 1.0% crystal violet and 0.5% glacial acetic acid in ethanol. Colonies of at least 50 cells were defined as surviving cells. Percentage of surviving colonies were calculated using the one-hit multi-target formula.

Micronucleus assay

The micronucleus (MN) number of BMSCs in each group was measured by Cytochalasin B assay after co-culturing for 24 h. Briefly, cells were cultured in medium with Cytochalasin B (0.25 mg/mL, Solarbio, China, Cat# 18w346) for 48 h, fixed with Carnoy's fluid for 15 min at room temperature, stained with acridine orange (30 mg/mL), and then observed by fluorescence microscopy. At least 500 binucleate cells were calculated for each group.

Immunofluorescence staining

The number of P53-binding protein-1 (53BP1) foci in each group at 0.5 h, 2 h, 6 h, 12 h, and 24 h of co-culturing was measured by immunofluorescence staining assay as reported previously [28]. Briefly, cells of each group were fixed in 4% polyformaldehyde for 15 min and permeabilized in PBS with 0.5% Triton-X 100. After blockage with 5% non-fat milk for 1 h, cells were incubated with mouse monoclonal anti-53BP1 antibody (Abcam, Cat# ab36823, UK) for 2 h at room temperature. After incubation with Alexa Fluor® 594 anti-mouse antibody (Molecular Probes, USA) for 1 h at room temperature, cells were counter-stained with DAPI (Invitrogen, Cat #P36941) and observed with a fluorescent microscope (Nikon, Tokyo, Japan). At least 100 cells were calculated in each group.

ELISA

The levels of TGF-β (human TGF-β1 ELISA Kit; Neobioscience Biotech Co., Ltd., Shenzhen, China; Cat# H150522-107b) and ROS (human ROS ELISA Kit; Westang Bio-tech Co., Ltd., Shanghai, China; Cat # F02471) in the conditioned medium and the culture supernatant of each group were detected by ELISA kits following the manufacturer's instructions.

Western blot

Cells at 6 h and 12 h of co-culturing were lysed in RIPA buffer (Beyotime, Cat# P0013C, China). Proteins were separated by 10% SDS-PAGE and transferred to a methanol-activated PVDF membrane (Millipore, Cat# IPVH00010, USA).The membrane was blocked for 1 h in PBST containing 5% milk and subsequently probed with p38 antibody (ImmunoWay, Cat# B6201, USA), JNK antibody (ImmunoWay, Cat# B4001,USA), ERK1/2 antibody (Cat# ImmunoWay, B2601, USA), cyclooxygenase-2 (COX-2) antibody (ImmunoWay, Cat#B7301, USA), phosphorylated p38 antibody (ImmunoWay, Cat# B4401, USA), phosphorylated JNK antibody (ImmunoWay, Cat# B6701,USA), phosphorylated ERK1/2 antibody (Immunollay, Cat#B0001, USA), and GAPDH antibody (Abcam, Cat# ab9485, USA) for 2 h. After 1 h incubation with goat-anti-mouse HRP-conjugated secondary antibody (Abcam, Cat# ab97051, USA), the protein bands were detected with luminal reagent (Millipore, Cat# WBKLS0500, USA). Their relative intensities were quantified using Adobe Photoshop software (Adobe Systems Inc., San Jose, USA).

Statistical analysis

Each *in vitro* experiment was repeated at least 3 times, and the data were analyzed by SPSS (v13.0). The statistical significance was calculated by one-way ANOVA or by the *t* test. $P<0.05$ was considered significant.

Results

Inhibitory effect of conditioned medium on cell viability of bystander cells and the protective effects of APS

To determine the effect of APS on cell viability of bystander cell BMSCs, CCK8 assay and cell colony formation assay were performed. The cell viability (Figure 1A) and percentage of surviving colonies cellular colony rate (Figure 1B) of bystander cell BMSCs was distinctly inhibited by conditioned medium ($P<0.05$) compared with the control group and APS group. There were no differences between the control group and APS medium group ($P>0.05$). Additionally, cell viability (Figure 1A) and percentage of surviving colonies (Figure 1B) of the APS+CM group was significantly higher than in the CM group ($P<0.05$). These data show that APS has protective effects on cell survival of bystander cells against conditioned medium.

Genomic instability of bystander cells induced by conditioned medium and the protective effects of APS

To investigate the effect of APS on genomic instability of BMSCs, MN formation and 53BP1 foci were measured. At 24 h after co-culturing, the MN frequency was significantly higher in the CM group than in the control group (Figure 2A) ($P<0.01$). Cellular MN frequency of the APS+CM group was significantly lower than that of the CM group ($P<0.05$), which indicates APS has a protective function in cellular MN formation in BMSCs treated by conditioned medium.
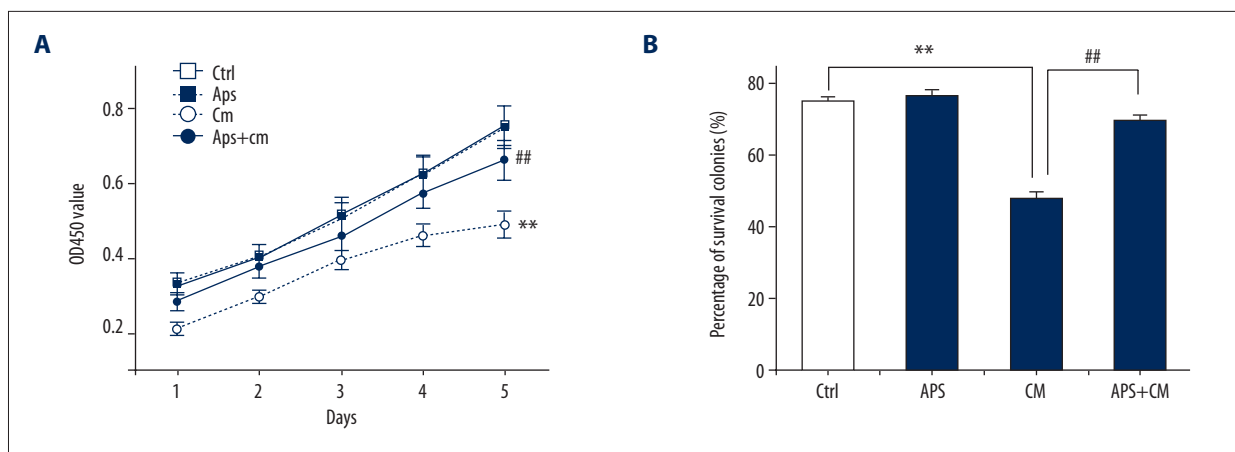
Figure 1. Analysis of the growth of the bystander BMSCs. BMSCs were divided into the control group, APS group, CM group, and APS+CM group. (**A**) Cell proliferation was detected with CCK-8 assay. (**B**) Colony formation by cells of each group. Compared with control group or APS group, * *P*<0.05, ** *P*<0.01. Compared with CM group, # *P*<0.05, ## *P*<0.01.
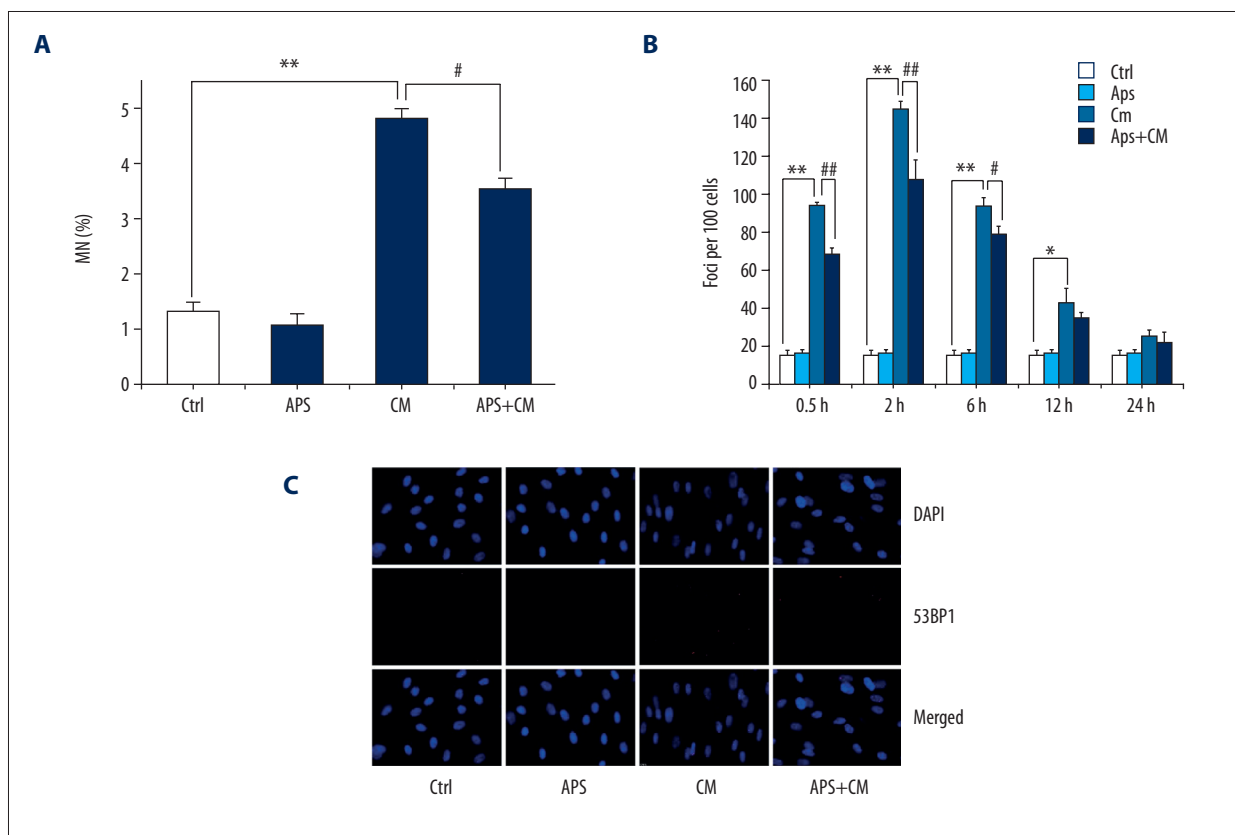

Figure 2. Genomic instability analysis of the bystander BMSCs. BMSCs were divided into the control group, APS group, CM group, and APS+CM group. (**A**) Frequency of micronuclei (MNF) in bystander cells at 24 h were calculated and compared. (**B**) The number of 53BP1 foci per 100 cells at indicated time points was calculated and compared. (**C**) Representative images of the 53BP1 foci in each group at 2 h. Compared with control group or APS group, * *P*<0.05, ** *P*<0.01. Compared with CM group, # *P*<0.05, ## *P*<0.01.
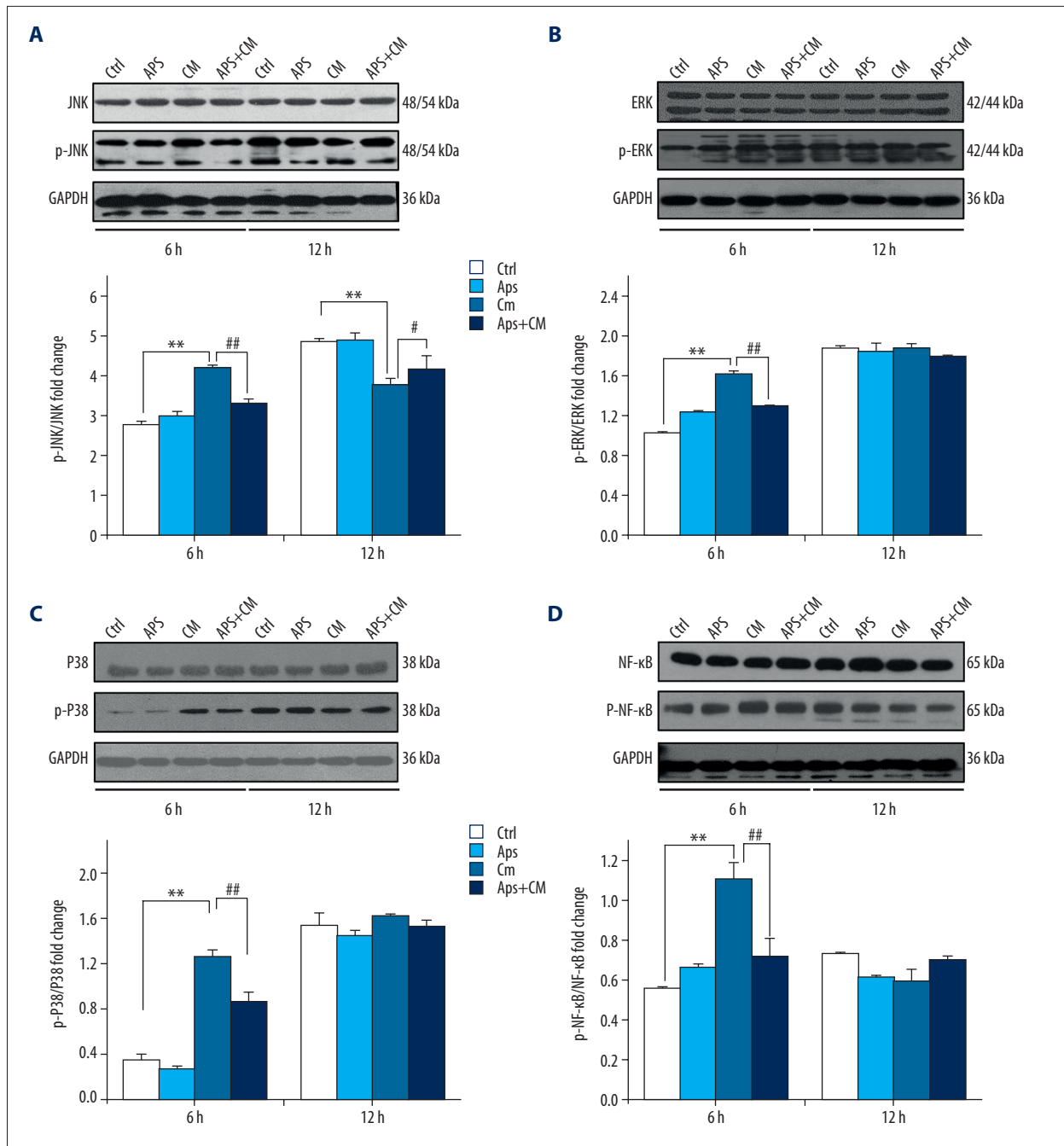
Figure 3. Analysis of protein levels in the bystander BMSCs. BMSCs were divided into the control group, APS group, CM group, and APS+CM group. Western blot was used to detect levels of JNK, p-JNK (**A**), ERK, p-ERK (**B**), P38, p-P38 (**C**) and, NF-κB, and p- NF-κB (**D**). Representative and quantitative Western blot results are shown, respectively. Compared with control group or APS group, * *P*<0.05, ** *P*<0.01. Compared with CM group, # *P*<0.05, ## *P*<0.01.

The 53BP1 foci, a widely used marker of DSBs, were measured at 0.5 h, 2 h, 6 h, 12 h, and 24 h of co-culturing (Figure 2B). In general, the 53BP1 foci number increased sharply from 0 h to 2 h, decreased gradually from 2 h to 24 h in bystander cells, and decreased to the control levels at 24 h. The 53BP1 foci numbers at each time point (0.5 h, 2 h, 6 h, and 12 h) were significantly higher in the CM group than in the control group (*P*<0.05). At 0.5 h, 2 h, and 6 h, the cellular 53BP1 foci number in the APS+CM group was significantly lower than that in the CM group (*P*<0.05). Figure 2C shows a representative image of the 53BP1 foci in each group at 2 h.
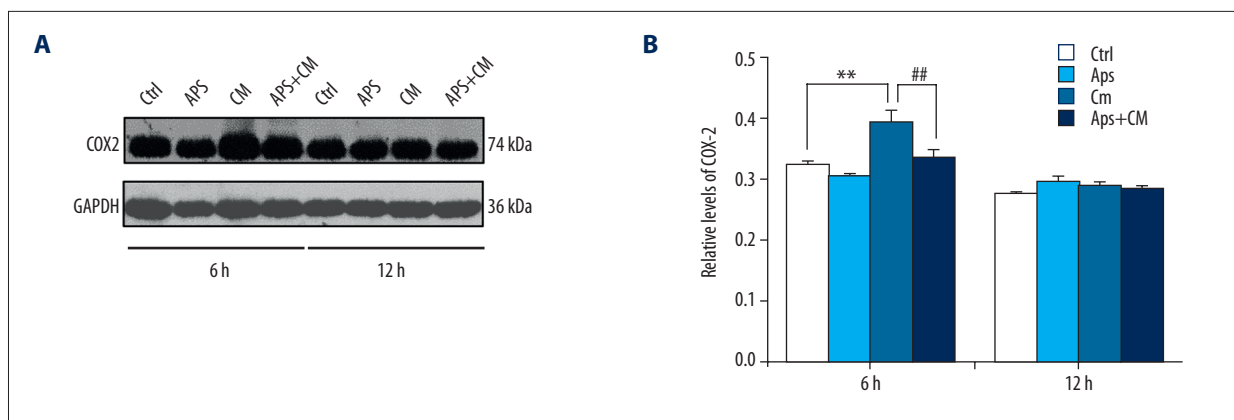
Figure 4. The COX-2 protein level in the bystander BMSCs. BMSCs were divided into the control group, APS group, CM group, and APS+CM group. Western blot was used to detect COX-2 level in bystander cells at 6 h and 12 h after co-culturing with conditioned medium and APS. Representative (**A**) and quantitative Western blot results (**B**) were shown, respectively. Compared with control group or APS group, * $P<0.05$, ** $P<0.01$. Compared with CM group, # $P<0.05$, ## $P<0.01$.

These results suggest that there is genomic instability in BMSCs and that APS has protective effects on cell genomic instability of bystander cells against conditioned medium.

The MAPK/NF-κB signal pathway is activated in bystander cells and APS regulates the protein expression of this pathway

To check whether MAPKs and NF-κB signaling pathways are involved in the RIBE in the BMSCs, the expressions of JNK, ERK, p38, and NF-κB were measured by Western blot. After treatment with conditioned medium, the levels of total JNK, ERK, P38, and NF-κB proteins were not obviously altered at 6 h or 12 h (Figure 3).

Reversible phosphorylation of proteins is an important regulatory mechanism that occurs in prokaryotic and eukaryotic organisms. Many enzymes and receptors are switched "on" or "off" by phosphorylation and dephosphorylation [29]. Next, we tested the phosphorylation levels of MAPKs-related protein and p-NF-κB (p-P65). As shown in Figure 3A, compared with the control group, the p-JNK/JNK fold change was increased, with a peak value at 6 h after treatment with conditioned medium and was downregulated at 12 h. Compared with the CM group, the APS+CM group significantly decreased the p-JNK/JNK fold change at 6 h but increased p-JNK/JNK fold change at 12 h (P<0.05). As shown in Figure 3B–3D, after treatment with conditioned medium, the p-ERK/ERK, p-P38/P38, and p-NF-κB/NF-κB fold change in the CM group was increased more at 6 h than in the control group (P<0.05). The APS+CM group had significantly decreased p-ERK/ERK, p-P38/P38, and p-NF-κB/NF-κB fold change than in the CM group (P<0.05). There was no significant change at 12 h.

These findings demonstrate that proteins in the MAPK and NF-κB signal pathways are in bystander cells and APS could regulate the level of these phosphorylated proteins.

The expression level of COX-2 increases in bystander cells and APS inhibits this increase

We further detected the expression of COX-2 by Western blot. The result showed that treatment with conditioned medium significantly increased the level of COX-2 at 6 h compared with the control group (P<0.05) (Figure 4A, 4B). APS reduced the protein expression of COX-2 at 6 h (P<0.05). There was no significant change at 12 h. Thus, APS could inhibit COX-2 expression induced by RIBE in bystander cells.

The relative concentrations of ROS and TGF-β

The levels of ROS and TGF-β were detected by ELISA. Figure 5A shows the relative concentrations of TGF-β in conditioned medium. After radiation, the concentrations of TGF-β in A549 supernatant were gradually increased from 0 h to 12 h. After radiation, the concentrations of ROS in A549 supernatant (Figure 5B) first increased sharply and then decreased gradually. At 3 h, the concentrations of ROS reached the peak. Thus, the conditioned medium at 3 h was collected. In the supernatant of the control group and APS group, the ROS level maintained at a baseline level (Figure 5C). In the CM group and APS+CM group, the ROS expression first increased and then decreased, and at 9 h the ROS expression reached the peak. CM group had significantly higher levels of ROS than in the control group or APS group at all detected time points (P<0.05). Compared with the CM group, APS+CM had significantly lower levels of ROS at 3 h, 6 h, and 9 h (P<0.05). These results show that the levels of ROS and TGF-β are increased in conditioned medium and the culture supernatant of bystander cells, and
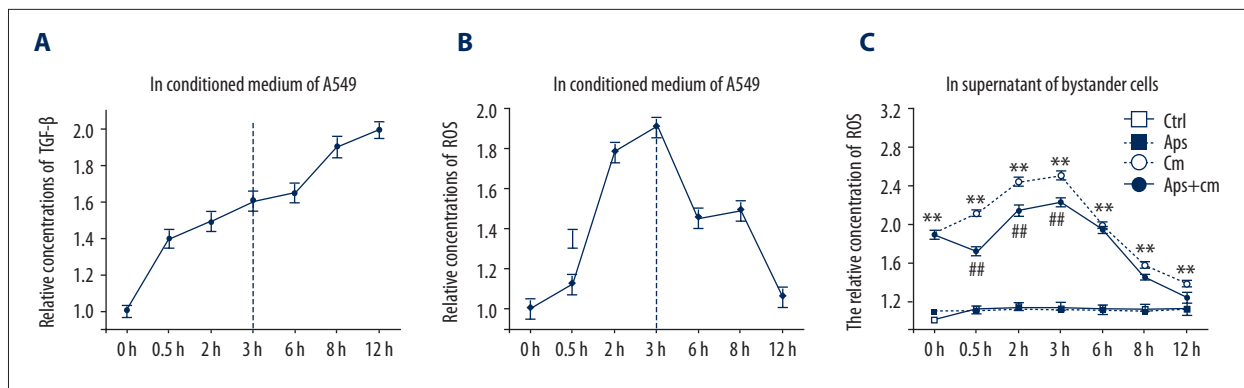
Figure 5. The levels of ROS and TGF-β in conditioned medium and in supernatant of the bystander BMSCs. The levels of ROS and TGF-β were detected by ELISA. The conditioned medium was harvested at 0 h, 0.5 h, 2 h, 3 h, 6 h, 8 h, and 12 h after exposure to X-rays. The supernatant of each experiment group was collected at 0 h, 3 h, 6 h, 9 h, 12 h, 15 h, and 18 h after co-culturing with conditioned medium. (**A**) The relative concentrations of TGF-β in conditioned medium. (**B**) The relative concentrations of ROS in conditioned medium. (C) The relative concentrations of ROS in supernatant of each experiment group. Compared with control group or APS group, * $P<0.05$, ** $P<0.01$. Compared with CM group, # $P<0.05$, ## $P<0.01$.

that APS can decrease the level of ROS in the culture supernatant of bystander cells.

Discussion

More than half of cancer patients undergo radiotherapy for treatment of cancer [30], especially lung cancer, which is a serious malignancy in China, with the highest morbidity and mortality [1]. However, RIBE may occur during radiotherapy [31,32]. One important consequence of RIBE is the DNA damage in bystander cells, such as DSB and MN formation, [33,34] which are known to induce genome destabilization. 53BP1 can activate the signaling pathways of DSB [35], which leads to cell-cycle delay, apoptosis, and senescence, and is critical for maintaining genomic stability. MN is a kind of abnormal structure in eukaryotic cells and is a form of chromosome aberration in interphase cells [36]; it is often caused by various physical and chemical factors, such as radiation and chemical agents. Thus, MN is a representative index for radiation damage. In the present study, the survival rate of bystander cells treated with conditioned medium was lower. The MN formation frequency and its 53BP1 foci number in bystander cells treated with conditioned medium were higher. This indicates that cell growth slows and the genomic instability is enhanced in bystander cells after treatment with conditioned medium. This is accordance with others studies [37,38]. In the present study, APS had protective effects on cell survival level of bystander cells against conditioned medium and maintained the stability of the genome through decreasing 53BP1 foci number and MN formation.

The MAPK pathway is an important pathway that is involved in radiation responses and mediates bystander cells [39]. The MAPK pathway plays a role in eliciting specific biological responses through transmitting stress signals from the cell surface to the nucleus [40] and is related to cellular events such as proliferation, senescence, differentiation, and apoptosis. [41–44]. Three primary MAPK families have been widely characterized: the ERK1/2 pathway, the C-Jun N-terminal kinase/stress-activated protein kinase (JNK/SAPK) pathway, and the p38 kinase pathway. MAPK can be activated in response to radiation-induced NF-κB activation and DNA damage [45] and activated in bystander cells by ROS released from activated radiation cells [46,47]. In the present study, the expression of phosphorylated p38, JNK, ERK1/2, and P65 proteins were increased in bystander effect cells treated with conditioned medium only at 6 h, which indicates that the MAPK/NF-κB pathway is activated in bystander cells at this time. This result is consistent with other reports [37,38,46]. After treatment with APS, p-ERK/ERK, p-P38/P38, and p-NF-κB/NF-κB fold change was decreased. These findings demonstrate that proteins in the MAPK and NF-κB signal pathways are activated in bystander cells and APS can regulate the level of these phosphorylated proteins.

COX-2, the inducible form of cyclooxygenase, is activated by growth factors and cytokines to catalyze the conversion of arachidonic acid to prostaglandins [48]. A previous study showed that COX-2 is an important mediator of bystander effects. P38/MAPK signaling pathways have been implicated in COX-2 upregulation [49]. COX-2 has an important role in modulating the inflammatory response [50], which is often associated with genomic instability and carcinogenesis [51]. Our study shows that COX-2 level was increased in bystander cells treated with conditioned medium only, indicating that COX-2 is invloved in RIBE. APS reduced the protein expression of COX-2 at 6 h, which may be related to the downregulation of the MAPK/NF-κB signal pathway.

ROS, downstream products of COX-2, is observed in stress, especially radiation stress, which can be released into medium by irradiated cells and then affects the bystander cells [52]. A high level of ROS may lead to increased DNA damage [53]. In the present study, ROS level in conditioned medium was first increased sharply and then decreased gradually and reach the peak at 3 h. Then, the conditioned medium at 3 h was collected and used to culture the bystander cells. Thus, the BMSCs could be stimulated by the ROS in the conditioned medium. TGF-β is sensitive to radiation stress [54] and is increased in a dose-dependent manner in irradiated rat liver [55]. It has been reported that TGF-β is directly involved in radiation responses [56]. Moreover, TGF-β has been found to be one of the RIBE mediators [57–59]. For example, TGF-β is related to radiation-induced DSB [60] and may induce the release of ROS [57]. In the present study, we found that TGF-β level in conditioned medium were increased, which may activate the intracellular MAPK signaling pathway and increase the release of ROS in bystander cells. This is the other source of the ROS that stimulated BMSCs. So, both ROS transferred from conditioned medium and newly generated ROS in bystander cells could lead to increased DNA damage. We found that APS strongly inhibited the level of ROS in bystander cells, showing that APS can reduce oxidation level, as was also reported by Sun et al. [61].

Previous studies have shown that APS inhibits both the mitochondrial injury caused by the continuous production of free radicals and selective oxidative damage, which is commonly associated with fatigue [62,63]. APS is thought to protect mitochondrial function by scavenging ROS [61]. A previous study suggested that APS may be used as a new target in reducing hyperpigmentation through the ERK signal pathway [64] and can regulate the TLR4/NF-κB signaling pathway to inhibit cell damage caused by TNF-. In the present study, APS attenuated the growth inhibition of bystander cells and reduced genomic instability (such as alleviating MN and 53BP1 increase) induced by RIBE, which may be related to downregulation of the MAPK-related protein phosphorylation, COX-2 expression, and ROS level.

Conclusions

Our results demonstrate that RIBE in BMSCs is mediated by ROS in the conditioned medium released by irradiated A549 cells and by bystander BMSCs, which is induced through activation of MAPK/NF-κB pathways in BMSCs. APS blocks RIBE through regulating the MAPK/NF-κB pathway. The MAPK signaling pathway is probably one of mechanisms underlying
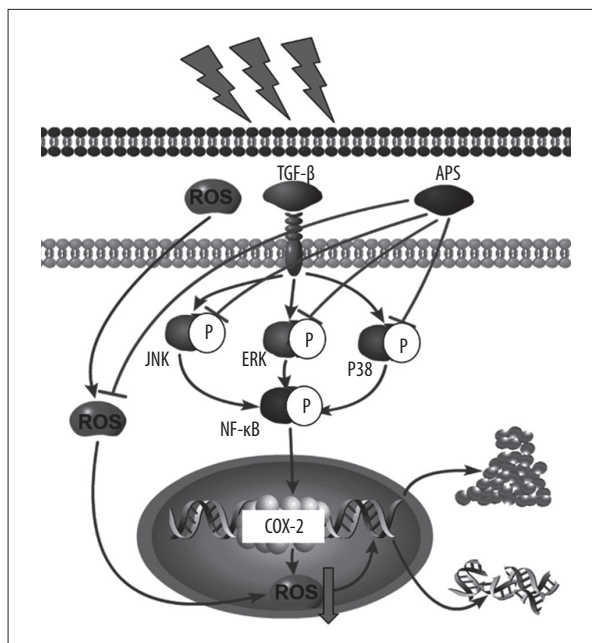

Figure 6. A model of RIBE in this study. In summary, the ROS delivered from irradiated cells and bystander cells can inhibit cell growth, induce DNA DSB, and cause genomic instability. The activated MAPK/NF-κB pathways synergistically increase cellular injury. APS might block RIBE through regulating the MAPK/NF-κB pathway.

the anti-RIBE of APS (Figure 6). ROS released by the irradiated cells and the bystander cells can inhibit cell growth, induce DNA DSB, and cause genomic instability. The activated MAPK pathway synergistically increases cellular injury. APS might decrease RIBE through regulating the MAPK/NF-κB pathway. Our findings may provide experimental evidence for the use of APS in the prevention of RIBE during radiotherapy for lung cancer.

Conflicts of interest

None.

References:

1. Chen W, Zheng R, Baade P et al: Cancer statistics in China 2015. Cancer J Clin, 2016; 66: 115–32

2. Jerzy B, Jonathan M, Katarzyna W et al: Bystander effects of nitric oxide in anti-tumor photodynamic therapy. Cancer Cell Microenviron, 2017; 4: e1511

3. Nagasawa H, Little J: Induction of sister chromatid exchanges by extremely low doses of alpha-particles. Cancer Res, 1992; 52: 6394–96

4. Schaue D, Micewicz E, Ratikan J et al: Radiation and inflammation. Semin Radiat Oncol, 2015; 25: 4–10

5. William F, Morgan, Marianne B et al: Non-targeted effects induced by ionizing radiation: Mechanisms and potential impact on radiation induced health effects. Cancer Lett, 2015; 356: 17–21

6. Yang H, Asaad N, Held K: Medium-mediated intercellular communication is involved in bystander responses of X-ray-irradiated normal human fibroblasts. Oncogene, 2005; 24: 2096–103

7. Kadhim M, Macdonald D, Goodhead D et al: Transmission of chromosomal instability after plutonium alpha particle irradiation. Nature, 1992; 355: 738–40

8. Mothersill C, Seymour C: Medium from irradiated human epithelial cells but not human fibroblasts reduces the clonogenic survival of unirradiated cells. Int J Radiat Biol, 1997; 71: 421–27

9. Sawant S, Randers G, Geard C et al: The bystander effect in radiation oncogenesis: I. Transformation in C3H 10T1/2 cells *in vitro* can be initiated in the unirradiated neighbors of irradiated cells. Radiat Res, 2001; 155: 397–401

10. Wu X, Wang Z, Qian M et al: Adrenaline stimulates the proliferation and migration of mesenchymal stem cells towards the LPS-induced lung injury. J Cell Mol Med, 2014; 18: 1612–22

11. Sally M, Amal S, Somia H et al: Mesenchymal stromal cell injection protects against oxidative stress in *Escherichia coli* – induced acute lung injury in mice. Cytotherapy, 2014; 16: 764–75

12. Sara R, Annika A, Ingrid S et al: MSC from fetal and adult lungs possess lung-specific properties compared to bone marrow-derived MSC. Sci Rep, 2016; 6: 29160

13. Gutierrez F, Rodriguez F, Ramos C et al: Effects of intravenous administration of allogenic bone marrow-and adipose tissue-derived mesenchymal stem cells on functional recovery and brain repair markers in experimental ischemic stroke. Stem Cell Res Ther, 2013; 4: 11–15

14. Sonomoto K, Yamaoka K, Tanaka Y: An approach to bone and cartilage repair of rheumatoid arthritis by mesenchymal stem cells. J UOEH, 2014; 36: 141–46

15. Noronha J, Correia P: Mesenchymal stem cells ageing: targeting the "purinome" to promote osteogenic differentiation and bone repair. J Cell Physiol, 2016; 231: 1852–61

16. Wong S, Rowley J, Redpath A et al: mesenchymal stem cells and their contributions to tissue repair. Pharmacol Therapeut, 2015; 151: 107–20

17. Liu C, Chen Z, Chen Z et al: Multiple tumor types may originate from bone-marrow-derived cells. Neoplasia, 2006; 8: 716–24

18. Shain K, Yarde D, Meads M et al: Beta1 integrin adhesion enhances IL-6-mediated STAT3 signaling in myeloma cells: implications for micro-environment influence on tumor survival and proliferation. Cancer Res 2009;69: 1009-15.

19. Wang N, Liu J, Xie F, et al. miR-124/ATF-6, a novel lifespan extension pathway of *Astragalus polysaccharide* in *Caenorhabditis elegans*. J Cell Biochem, 2015; 116: 242–51

20. Yin X, Chen L, Liu Y et al: Enhancement of the innate immune response of bladder epithelial cells by *Astragalus polysaccharides* through upregulation of TLR4 expression. Biochem Biophys Res Commun, 2010; 397: 232–38

21. Mao X, Yu F, Wang N et al: Hypoglycemic effect of polysaccharide enriched extract of *Astragalus membranaceus* in diet induced insulinresistant C57BL/6J mice and its potential mechanism. Phytomedicine, 2009; 16: 416–25

22. Yao C, Gao F, Chen Y et al: [Experimental research of *Astragalus polysaccharides* collagen sponge in enhancing angiogenesis and collagen synthesis.] Zhongguo Xiu Fu Chong Jian Wai Ke Za Zhi, 2011; 25: 1481–85 [in Chinese]

23. Lu J, Chen X, Zhang Y et al: *Astragalus polysaccharide* induces antiinflammatory effects dependent on AMPK activity in palmitate-treated RAW264.7 cells. Int J Mol Med, 2013; 31: 1463–70

24. Zhang YW, Wu CY, Cheng JT: Merit of *Astragalus polysaccharide* in the improvement of early diabetic nephropathy with an effect on mRNA expressions of NF-kappa B and I kappa B in renal cortex of strep tozotoxin-induced diabetic rats. J Ethnopharmacol, 2007; 114: 387–92

25. Li S, Zhang Y, Zhao J: Preparation and suppressive effect of astragalus polysaccharide in glomerulonephritis rats. Int Immunopharmacol, 2007; 7: 23–28

26. Yang F, Yan G, Li Y et al: *Astragalus polysaccharide* attenuated iron overload-induced dysfunction of mesenchymal stem cells via suppressing mitochondrial ROS. Cell Physiol Biochem, 2016; 39: 1369–79

27. Chen J, Hu J, Zhang J et al: [Effect of astragalus polysaccharides on expression of Bcl-2 in human hepatoma cell lines Hep G2.] Chinese Journal of Gerontology, 2014; 34: 124–26 [in Chinese]

28. He J, Li J, Ye C et al: Cell cycle suspension: A novel process lurking in G(2) arrest. Cell Cycle, 2011; 10: 1468–76

29. Vlastaridis P, Kyriakidou P, Chaliotis A et al: Estimating the total number of phosphoproteins and phosphorylation sites in eukaryotic proteomes. Gigascience, 2017; 6: 1–11

30. Ferlay J, Shin H, Bray F et al: Estimates of worldwide burden of cancer in 2008: GLOBOCAN 2008. Int J Cancer, 2010; 127: 2893–917

31. Prise K, Sullivan J: Radiation-induced bystander signalling in cancer therapy. Nat Rev Cancer, 2009; 9: 351–60

32. Whiteside J, McMillan T: A bystander effect is induced in human cells treated with UVA radiation but not UVB radiation. Radiat Res, 2009; 171: 204–11

33. Smilenov L, Hall E, Bonner W, Sedelnikova O: A microbeam study of DNA double-strand breaks in bystander primary human fibroblasts. Radiat Prot Dosimetry, 2006; 122: 256–59

34. Soleymanifard S, Bahreyni M, Kamran R et al: Comparison of radiation-induced bystander effect in QU-DB cells after acute and fractionated irradiation: An *in vitro* study. Cell J, 2016; 18: 346–52

35. Zhou H, Randers G, Suzuki M et al: Genotoxic damage in non-irradiated cells: Contribution from the bystander effect. Radiat Prot Dosimetry, 2002; 99: 227–32

36. Shah A, Lakkad B, Rao M: Genotoxicity in lead treated human lymphocytes evaluated by micronucleus and comet assays. Indian J Exp Biol, 2016; 54: 502–8

37. Li L, Wang L, Prise KM et al: Akt/mTOR mediated induction of bystander effect signaling in a nucleus independent manner in irradiated human lung adenocarcinoma epithelial cells. Oncotarget, 2017; 8: 18010–20

38. Nelson G, Kucheryavenko O, Wordsworth J, von Zglinicki T: The senescent bystander effect is caused by ROS-activated NF-κB signaling mechanisms of ageing and development. Mech Ageing Dev, 2018; 170: 30–36

39. Ivanov V, Zhou H, Ghandhi S et al: Radiation-induced bystander signaling pathways in human fibroblasts: A role for interleukin-33 in the signal transmission. Cell Signal, 2010; 22: 1076–876

40. Asur R, Balasubramaniam M, Marples B et al: Involvement of MAPK proteins in bystander effects induced by chemicals and ionizing radiation. Mutat Res, 2010; 686: 15–29

41. Lioni M, Noma K, Snyder A et al: Bortezomib induces apoptosis in esophageal squamous cell carcinoma cells through activation of the p38 mitogen-activated protein kinase pathway. Mol Cancer Ther, 2008; 7: 2866–75

42. Xie J, Xu L, Xie Y et al: Roles of ezrin in the growth and invasiveness of esophageal squamous carcinoma cells. Int J Cancer, 2009; 124: 2549–58

43. Bragado P, Armesilla A, Silva A, Porras A: Apoptosis by cisplatin requires p53 mediated p38alpha MAPK activation through ROS generation. Apoptosis, 2007; 12: 1733–42

44. Zhu L, Liu YJ, Shen H et al: Astragalus and baicalein regulate inflammation of mesenchymal stem cells (MSCs) by the mitogen-activated protein kinase (MAPK)/ERK pathway. Med Sci Monit, 2017; 23: 3209–16

45. Havaki S, Kotsinas A, Chronopoulos E et al: The role of oxidative DNA damage in radiation induced bystander effect. Cancer Lett, 2015; 356: 43–51

46. Ki Y, Park J, Lee J et al: JNK and p38 MAPK regulate oxidative stress and the inflammatory response in chlorpyrifos-induced apoptosis. Toxicol Lett, 2013; 218: 235–45

47. Deschênes X, Gaumont M, Bourdeau V et al: Tumor suppressor activity of the ERK/MAPK pathway by promoting selective protein degradation. Genes Dev, 2013; 27: 900–15

48. Subbaramaiah K, Chung W, Dannenberg A: Ceramide regulates the transcription of cyclooxygenase-2 Evidence for involvement of extracellular signal-regulated kinase/c-Jun N-terminal kinase and p38 mitogen-activated protein kinase pathways. J Biol Chem, 1998; 273: 32943–49

49. Zhou H, Ivanov V, Gillespie J et al: Mechanism of radiation-induced bystander effect: Role of the cyclooxygenase-2 signaling pathway. Proc Natl Acad Sci USA, 2005; 102: 1464–66

50. Zhao Y, de Toledo SM, Hu G et al: Connexins and cyclooxygenase-2 crosstalk in the expression of radiation-induced bystander effects. Br J Cancer, 2014; 111: 125–31

51. Acheva A, Schettino G, Prise KM: Pro-inflammatory signaling in a 3D organotypic skin model after low LET irradiation-NF-κB COX-2 activation and impact on cell differentiation. Front Immunol 2017; 8: 82

52. Kazemi E, Mortazavi S, Ali-Ghanbari A et al: Effect of 900 MHz electromagnetic radiation on the induction of ROS in human peripheral blood mononuclear cells. J Biomed Phys Eng, 2015; 5: 105–14

53. Sokolov M, Dickey J, Bonner W et al: Gamma-H2AX in bystander cells: Not just a radiation-triggered event, a cellular response to stress mediated by intercellular communication. Cell Cycle, 2007; 6: 2210–12

54. Andarawewa KL, Paupert J, Pal A et al: New rationales for using TGFbeta inhibitors in radiotherapy. Int J Radiat Biol, 2007; 83: 803–11

55. Anscher MS, Crocker IR, Jirtle RL: Transforming growth factor-beta 1 expression in irradiated liver. Radiat Res, 1990; 122: 77–85

56. Kirshner J, Jobling MF, Pajares MJ et al: Barcellos-Hoff MH.Inhibition of transforming growth factor-beta1 signaling attenuates ataxia telangiectasia mutated activity in response to genotoxic stress. Cancer Res, 2006; 66: 10861–69

57. Jiang Y, Chen X, Tian W et al: The role of TGF-β1-miR-21-ROS pathway in bystander responses induced by irradiated non-small-cell lung cancer cells. Br J Cancer, 2014; 111: 772–80

58. Temme J, Bauer G: Low-dose gamma irradiation enhances superoxide anion production by nonirradiated cells through TGF-β 1-dependent bystander signaling. Radiat Res, 2013; 179: 422–32

59. Iyer R, Lehnert BE, Svensson R: Factors underlying the cell growth-related bystander responses to alpha particles. Cancer Res, 2000; 60: 1290–98

60. Wang M, Saha J, Hada M et al: Novel Smad proteins localize to IR-induced double-strand breaks: Interplay between TGFβ and ATM pathways. Nucleic Acids Res, 2013; 41: 933–42

61. Sun Q, Jia N, Wang W et al: Protective effects of astragaloside IV against amyloid beta1-42 neurotoxicity by inhibiting the mitochondrial permeability transition pore opening. PLoS One, 2014; 9: e98866

62. Li X, Zhang Y, Kuang H et al: Mitochondrial protection and anti-aging activity of Astragalus polysaccharides and their potential mechanism. Int J Mol Sci, 2012; 13: 1747–61

63. Lee SY, Tsai WC, Lin JC et al: Astragaloside II promotes intestinal epithelial repair by enhancing L-arginine uptake and activating the mTOR pathway. Sci Rep, 2017; 7: 12302

64. Tsao YT, Kuo CY, Kuan YD et al: The extracts of *Astragalus membranaceus* inhibit melanogenesis through the ERK signaling pathway. Int J Med Sci, 2017; 14: 1049–53